

A Data-driven Movement Model for Single Cellphone-based Indoor Positioning

Harshvardhan Vathsangam
Department of Computer Science
University of Southern California
Los Angeles, USA
vathsang@usc.edu

Anupam Tulsyan
Department of Computer Science
University of Southern California
Los Angeles, USA
tulsyan@usc.edu

Gaurav S. Sukhatme
Department of Computer Science
University of Southern California
Los Angeles, USA
gaurav@usc.edu

Abstract—Indoor localization is a promising area with applications in in-home monitoring and tracking. Fingerprinting and propagation model-based WiFi localization techniques have limited spatial resolution because of grid or graph-based representations. An alternative is to incorporate dynamics models based on real-time sensing of human movement and fuse these with WiFi measurements. We present a data-driven dynamic model that tracks the inherent periodicity in walking and converts this representation into velocity. This model however is prone to drift. We correct this drift with WiFi measurements to obtain a combined position estimate. Our approach records and fuses human body movement with WiFi positioning using a single mobile phone. We characterize the movement model to obtain an estimate of error predictions. The movement model showed a best case average RMS prediction error of .25 m/s. We also present a preliminary study characterizing combined system performance across straight line and L-shaped trajectories. The framework showed lower errors across the L-shaped trajectories (mean error ≈ 4.8 m using movement sensing versus a mean error ≈ 6 m without movement sensing) because of the ability assess the validity of a WiFi measurement. Higher errors were observed across the straight line trajectory due to imprecise trajectories.

Index Terms—Accelerometer, Indoor Localization, Mobile Phone, WiFi

I. INTRODUCTION

The need for cost-effective yet ubiquitous solutions brought on by rapidly ageing populations have led to the requirement of in-home monitoring. Accurate in-home monitoring requires the superimposition of relevant physiological information on an indoor spatial map. Attaching a spatial context to each physiological measure provides valuable information to clinical researchers developing intervention measures. The challenge is to be able to provide this while taking advantage of minimal or existing infrastructure. One set of promising candidates to provide this information are WiFi Received Signal Strength (RSS) based indoor localization techniques [1]. The two primary methods of location determination from WiFi involve signal strength propagation models [2] or data-driven fingerprinting techniques [1]. Fingerprinting techniques, in particular probabilistic versions [3, 4], have been reported to perform more accurately than propagation model based techniques.

WiFi fingerprinting techniques build sensor models by dividing floor space into grid cells [5] or nodes connected by a graph [6]. Measurement probabilities are then constructed for each location. The final a posteriori probability of a location given a measurement represents (at best) the probability of only a specific point (the center of the grid cell or the node position in the graph). Higher spatial resolution within each grid or around a node is limited by the nature of the representation. Existing solutions have attempted to mitigate this by

incorporating movement models that provide a trajectory of the user in the absence of WiFi measurements. Typical techniques include sliding windows [1] and Markov models [5] or Viterbi-like algorithms [7]. These approaches do not take advantage of on-body movement information.

Another approach is to physically sense user movement and fuse short term trajectories from on-body inertial sensors such as accelerometers and magnetometers [8] with long term corrections from WiFi RSS measurements. Typical approaches include foot-mounted inertial sensors to detect steps and direction and filters (Kalman Filters, Extended Kalman Filters [9] and particle filters [10]). These techniques still require external hardware on shoes. A more practical option is to sense movement and WiFi measurements with a single device. In-built movement sensors (such as accelerometers and gyroscopes) on mobile phones are the prime candidate for such an approach. Mobile phones are by far the most ubiquitous body-worn devices in the world today and already possess the required sensors for on-body movement sensing and WiFi localization. Common techniques using accelerometers involve measuring the number of zero-crossings of vertical acceleration signals [11] or signals above a certain threshold [12] to obtain step counts and correlating these to speed. These techniques are prone to errors imposed by improper mounting of the phone, incorrect calibration caused by differing walking styles or variance in signal magnitude. We adopt an alternative approach by taking advantage of the inherent cyclic nature in walking through a Fourier transform of accelerometer signals and converting these to distance moved.

In this paper, we present a data-driven probabilistic regression-based movement model fused with WiFi fingerprinting for indoor, phone-based positioning. We choose one example dynamic activity, walking because it is the most common dynamic activity in everyday living. In Sec. II-B we describe the WiFi fingerprinting technique used for indoor mobile positioning. In Sec. II-C, we show how one can build and use data-driven movement models to track user position. Such movement predictions are prone to drift but are corrected using WiFi as shown in Sec. II-D. Finally in Sec. III we present quantitative and qualitative results characterizing the movement model and the effect of augmenting WiFi with inertial information. Our approach is unique in that we use a single on-body device to extract and fuse short-term movement and long-term WiFi information using only data-driven techniques. We do not require precision mounting of the device.

II. SYSTEM DESIGN

Our approach predicts indoor positions for walking with two different sensing modalities - long term, low-resolution predictions with WiFi fingerprinting to obtain absolute position and short term trajectory predictions by estimating walking speed (and therefore displacement) using movement information from on-phone inertial sensors. These are then fused in a Kalman filter framework to obtain a complete estimate.

A. Hardware

We use HTC Nexus one running Android 2.2.1 for all our experiments. It features 802.11 b/g/n WiFi capabilities (operating at frequency, $F_{wifi} \approx 1$ Hz), accelerometer and orientation sensors (operating at frequency, $F_s \approx 33$ Hz). In our experiments, the phone is always worn on the left iliac crest via a custom belt-harness.

B. Basic Indoor Mobile Positioning with WiFi

Indoor positioning with WiFi involves measuring received signal strength values from one or more access points (APs) and using this information to infer position. A probabilistic (or Bayesian) approach [3, 4] was adopted over deterministic methods [1] because it provided a confidence estimate of predictions and thus a natural ability to handle uncertainty.

The probabilistic fingerprinting technique has two stages. The first stage involves building a sensor model to identify the probability of a certain RSS measurement given each candidate location. Given a set of N access points (AP_1, AP_2, \dots, AP_N), each location receives a radio signal with a certain power from each of the access points. Let these RSS measurements be defined as a tuple, $\mathbf{Z} = (z_1, z_2, \dots, z_N)$. The probabilistic technique defines a probability distribution for these measurements for each location as:

$$p(\mathbf{Z}|\mathbf{loc}_j) = p(z_1, z_2, \dots, z_N|\mathbf{loc}_j) \quad (1)$$

For simplicity, we assume that individual measurements are independent of each other given the location [3]. Therefore, the probability distribution becomes:

$$p(\mathbf{z}|\mathbf{loc}_j) = p(z_1|\mathbf{loc}_j)p(z_2|\mathbf{loc}_j)\dots p(z_N|\mathbf{loc}_j) \quad (2)$$

Thus for each location, we build a sensor model which is the probability of a RSS measurement tuple given the location. This is done by collecting RSS data for each location and fitting a probability model $p(z_i|\mathbf{loc}_j)$ for each access point AP_i for each location \mathbf{loc}_j . In this study, the probability distributions for RSS readings were multimodal, hence they were represented by a histogram.

The second stage involves determining the most likely position given a certain RSS measurement tuple measured for sample k , $\mathbf{z}(k)$. This is defined by a distribution across all locations where each location has the probability $p(\mathbf{loc}_j|\mathbf{z}(k))$. Using Bayes rule this can be expressed by the posterior distribution:

$$p(\mathbf{loc}_j|\mathbf{z}(k)) = \frac{p(\mathbf{z}(k)|\mathbf{loc}_j)p(\mathbf{loc}_j)}{\sum_{\mathbf{loc} \in \mathcal{L}} p(\mathbf{z}(k)|\mathbf{loc}_j)p(\mathbf{loc}_j)} \quad (3)$$

where each $p(\mathbf{z}(k)|\mathbf{loc}_j)$ is given by $p(\mathbf{z}(k)|\mathbf{loc}_j) = \prod_{i=1}^N p(z_i(k)|\mathbf{loc}_j)$, $p(\mathbf{loc}_j)$ is the prior distribution and \mathcal{L} is the set of all possible location values. Successive measurement tuples can thus be updated recursively using this technique

using the location distribution from the previous step as the prior in the next step. The final estimate of position was chosen as the maximum a posteriori (MAP) estimate of the posterior distribution. This corresponds to the location which has the highest probability. The final output is the tuple $[x_{RSS} \ y_{RSS}]^T$ which is the MAP estimate of the grid center.

C. Estimating Walking Speed from Inertial Sensors

An issue with WiFi fingerprinting is that unusual signal fluctuations can introduce unexpected jumps in final trajectory. This can be countered by making short term predictions and using a filter to smooth out position values. This requires a movement model to predict user trajectories. We describe a walking speed prediction algorithm that is used to make short term projections of user position.

1) *Capturing human walk*: Human walk can be modeled as a periodic motion [13]. We capture this periodicity using the frequency content of windowed acceleration signals with Fourier transforms. To demonstrate the ability of accelerometers to capture the periodicity of walk, a participant walked in tune with a metronome. The phone was worn on the left hip and streaming acceleration signals were captured. This was repeated for a range of metronome frequencies between 96 and 120 beats per minute (bpm). Fig. 1 illustrates the results of this experiment. The top panel indicates the Fourier transform of the X-axis acceleration stream for a beat frequency of 120 bpm. Similar plots exist for the Y and Z axes. We do not include these for brevity. Regular peaks can be seen indicative of dominant periodicities. The bottom panel depicts the variation of peaks of similar Fourier transforms for all metronome settings through a spectrogram plot. The dominant periodicities as captured by the phone accelerometer were found to vary with speed. Further, when the most dominant peak for each Fourier transform (obtained from a particular metronome setting) was plotted against metronome frequency, a perfect linear correlation (Pearson's coefficient, $r_{xy} = 1$) was observed.

Given this observation, each of the accelerometer data streams were divided into 10 second windows. For each window, the first sample was discarded and the new sample was appended in the end. Within each window, the 1024 point FFT was calculated for each stream. These parameters were determined from previous research [14]. For the sake of compactness of representation, FFT values for frequencies greater than 15 Hz were not used. This is based on the fact that everyday human body movements usually lie between 0.1 and 10 Hz [15]. The optimal window size must be chosen so that it is large enough to capture signal periodicity and short enough to not pick up long term variations in step frequency. The three FFT vectors corresponding to three axes are then concatenated to obtain a representation of walking.

2) *Mapping frequency spectrum of signals to speeds*: A linear [16], probabilistic model mapping the frequency content of walk to speed was assumed. This was achieved using Bayesian Linear Regression (BLR), a parametric, probabilistic interpretation of linear regression. Our approach builds on similar results obtained for determining speed of treadmill walking [14]. This approach is similar to that of Sun et. al [17] in that we train a linear model from frequency features to the target quantity, speed and then use this model to predict speeds for unseen data points. However, we adopt a

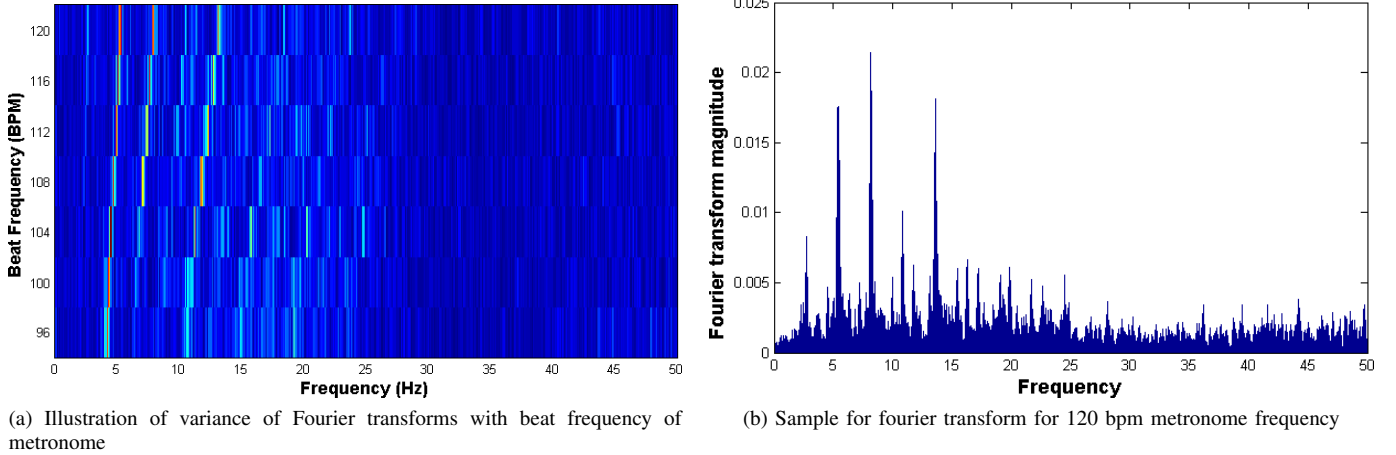


Figure 1: To demonstrate the ability of the accelerometers to capture the periodicity of walk, a participant walked in tune with a metronome for 20 seconds. The phone was worn on the left hip. This was repeated for a range of metronome frequencies from 96 to 120 beats per minute (bpm). The right panel indicates the Fourier transform of a when the participant walked to a beat frequency of 120 bpm. Regular peaks can be seen indicative of dominant periodicities. The bottom panel depicts similar Fourier transforms for all metronome settings. The dominant periodicities as captured by the phone accelerometer were found to vary with speed. Further, the most dominant peak for each Fourier transform obtained with each metronome setting was perfectly correlated with the metronome beat frequency ($r_{xy} = 1$)

probabilistic approach to this functional mapping. The use of probabilistic techniques incorporates the effects of noise thus guarding against overfitting and helps assess the confidence of a prediction. This confidence forms an important input when data from WiFi and inertial sensors are fused. Our approach maintains a constant-sized sample buffer containing 10 seconds of triaxial data and extract features from this buffer.

Consider a set of K -dimensional frequency feature inputs, $\mathbf{F} = \{x_i\}$, $i = 1, 2, \dots, N$ each of which are mapped to a corresponding target value: $\mathbf{V} = \{v_i\}$, $i = 1, 2, \dots, N$. In this study, the target quantity $\mathbf{V} = \{v_i\}_{i=1}^N$ was the speed reading as output by ground truth described in Sec. III-A. The input data points, $\mathbf{F} = \{x_i\}_{i=1}^N$, were the feature vectors computed using methods described in Sec. II-C1. The linear regression problem is to find the optimal parameter set \mathbf{w} such that:

$$v_i = \mathbf{w}^T f_i + \epsilon_i, \epsilon_i \sim \mathcal{N}(0, \beta^{-1}), \text{ or} \quad (4)$$

$$\mathbf{v} = \mathbf{W}^T \mathbf{F} + \epsilon, \epsilon \sim \mathcal{N}(\mathbf{0}, \beta^{-1} \mathbf{I}) \quad (5)$$

where β represents the noise variance parameter. For a Gaussian noise model, we can also obtain the conditional posterior distribution of the mapping \mathbf{V} given the input data points \mathbf{F} , $p(\mathbf{V}|\mathbf{F})$ as:

$$p(\mathbf{V}|\mathbf{F}) = \mathcal{N}(\mathbf{V}|\mathbf{w}^T \mathbf{F}, \beta^{-1} \mathbf{I}) \quad (6)$$

BLR adopts a Bayesian approach to the treatment of linear regression by fixing a prior over the parameter space \mathbf{w} as opposed to a definite value. Specifically, choosing a Gaussian prior over \mathbf{w} , $p(\mathbf{w}) = \mathcal{N}(\mathbf{w}|\mathbf{0}, \alpha^{-1} \mathbf{I})$. Using properties of Gaussians and Eq. 6 we obtain the posterior distribution of the parameter set as:

$$p(\mathbf{w}|\mathbf{V}) = \mathcal{N}(\mathbf{w}|\mathbf{m}_N, \mathbf{S}_N) \quad (7)$$

$$\mathbf{m}_N = \mathbf{S}_N \beta \mathbf{F}^T \mathbf{V} \quad (8)$$

$$\text{and } \mathbf{S}_N^{-1} = \alpha \mathbf{I} + \beta \mathbf{F}^T \mathbf{F} \quad (9)$$

In a fully Bayesian approach we adopt priors over α and β as well. We then follow an iterative approach to find the best hyperparameters α, β to maximize the evidence function for our dataset [18], find the best parameters $\hat{\mathbf{w}}$ to maximize

likelihood and repeating the same until convergence of the likelihood function. The optimal prediction for a new data point \mathbf{F}_{new} is:

$$p(\mathbf{V}_{new}|\mathbf{F}_{new}) = \mathcal{N}(\mathbf{V}_{new}|\hat{\mathbf{w}}^T \mathbf{F}_{new}, \beta^{-1} \mathbf{I}) \quad (10)$$

Extracting velocity from speed: For each new triaxial sample, given the accelerometer sampling frequency of F_s , corresponding to a inter-sample time of $\Delta T = \frac{1}{F_s}$, BLR provides an estimate of distance travelled within time ΔT . Let the speed as predicted by the BLR algorithm after the arrival of a sample numbered k be $v(k)$. Given a compass measurement that provides an absolute angle measurement, θ with respect to the magnetic north velocity vector for that time instant is $[v_{x,BLR}(k) \ v_{y,BLR}(k)]^T = [v_t \cos(\theta - \theta_0) \ v_t \sin(\theta - \theta_0)]^T$ where θ_0 is the building offset from the magnetic north. In our experiment, $\theta_0 \approx 260^\circ$. In practice, compass readings are prone to local fluctuations in magnetic field. This was partially mitigated by using low pass filtered versions of $\cos(\theta - \theta_0)$ and $\sin(\theta - \theta_0)$. Let $k = \cos(\theta - \theta_0)$. The filtered value was: $k_{filt} = \alpha k_{filt,previous} + (1 - \alpha)k$. The typical value of α was $\approx 0.9-0.95$. The lowpass filter was meant to provide stable readings of angle measurements by countering local fluctuations in magnetic field. In the future we plan on using gyroscopic and compass information through an additional angle state in our filter. This was not possible in this study because the smartphones used did not yet have gyroscopes at the time of the study period.

D. Fusion of WiFi and Human Movement Models

Inertial and WiFi measurements were fused using a Kalman filter. Fig. 2 illustrates the complete sensor fusion framework. We used a linear Kalman filter to test algorithm feasibility. A Kalman filter models a discrete-time controlled process using the following linear stochastic difference equations for state $\mathbf{x}(k)$ and measurement $\mathbf{z}(k)$:

$$\mathbf{x}_k = \mathbf{A}\mathbf{x}(k-1) + \mathbf{B}\mathbf{u}(k) + \mathbf{n}(k) \quad (11)$$

$$\mathbf{z}(k) = \mathbf{H}\mathbf{x}(k) + \mathbf{v}(k) \quad (12)$$

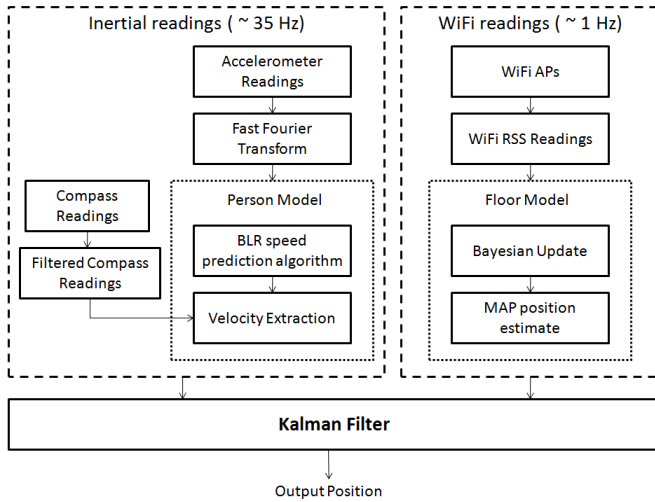


Figure 2: Illustration of the complete framework for trajectory prediction. Inertial and WiFi readings are fused using a Kalman filter. Inertial readings are converted to velocity measurements using the techniques outlined. Velocity measurements are used to propagate state (update step). For each WiFi reading, the location distribution is updated using Bayes rule and the MAP position estimate is taken from the distribution. This forms the correction (measurement step).

where \mathbf{A} , \mathbf{B} and \mathbf{H} are the transition and measurement processes. \mathbf{n} and \mathbf{v} are the process and measurement noise respectively. In this study, they are assumed to be independent, white, and with normal distributions $p(\mathbf{n}) \sim \mathcal{N}(\mathbf{0}, \mathbf{Q})$ and $p(\mathbf{v}) \sim \mathcal{N}(\mathbf{0}, \mathbf{R})$. \mathbf{Q} and \mathbf{R} are the state and measurement error covariance matrices. Parameters were defined as follows:

$$\mathbf{x}(k) = \begin{bmatrix} x(k) \\ y(k) \\ v_x(k) \\ v_y(k) \end{bmatrix}, \mathbf{A} = \begin{bmatrix} 1 & 0 & \Delta T & 0 \\ 0 & 1 & 0 & \Delta T \\ 0 & 0 & 0 & 0 \\ 0 & 0 & 0 & 0 \end{bmatrix},$$

$$\mathbf{z}(k) = \begin{bmatrix} x_{RSS}(k) \\ y_{RSS}(k) \end{bmatrix}, \mathbf{H} = \begin{bmatrix} 1 & 0 & 0 & 0 \\ 0 & 1 & 0 & 0 \end{bmatrix},$$

$$\mathbf{B}(k) = \mathbf{I}_{4 \times 4}, \mathbf{u}(k) = \begin{bmatrix} 0 \\ 0 \\ v_{x,BLR}(k) \\ v_{y,BLR}(k) \end{bmatrix}$$

where $x(k), y(k)$ are state positions, $v_x(k), v_y(k)$ are state velocities, $v_{x,BLR}(k), v_{y,BLR}(k)$ are velocities as obtained from the BLR algorithm and $x_{RSS}(k), y_{RSS}(k)$ are position estimates obtained from the Bayesian update. BLR also provides a variance estimate of velocity and this is fed into the \mathbf{Q} matrix for velocity estimates. WiFi was assumed to have a measurement error $\approx 5\text{m}$. In the current version of the filter we do not incorporate the geometry of the map. The prediction and correction steps are:

$$\hat{\mathbf{x}}^-(k) = \mathbf{A}\hat{\mathbf{x}}(k-1), \quad (13)$$

$$\mathbf{P}^-(k) = \mathbf{A}\mathbf{P}^-(k-1)\mathbf{A}^T + \mathbf{Q}, \quad (14)$$

$$\mathbf{K}(k) = \mathbf{P}^-(k)\mathbf{H}^T(\mathbf{H}\mathbf{P}^-(k)\mathbf{H}^T + \mathbf{R})^{-1}, \quad (15)$$

$$\hat{\mathbf{x}}(k) = \hat{\mathbf{x}}^-(k) + \mathbf{K}(k)(\mathbf{z}(k) - \mathbf{H}\hat{\mathbf{x}}^-(k)) \quad (16)$$

$$\mathbf{P}(k) = (\mathbf{I} - \mathbf{K}(k))\mathbf{P}^-(k) \quad (17)$$

where $\mathbf{P}^-(k)$ and $\mathbf{P}(k)$ are the apriori and aposteriori covariance matrices respectively.

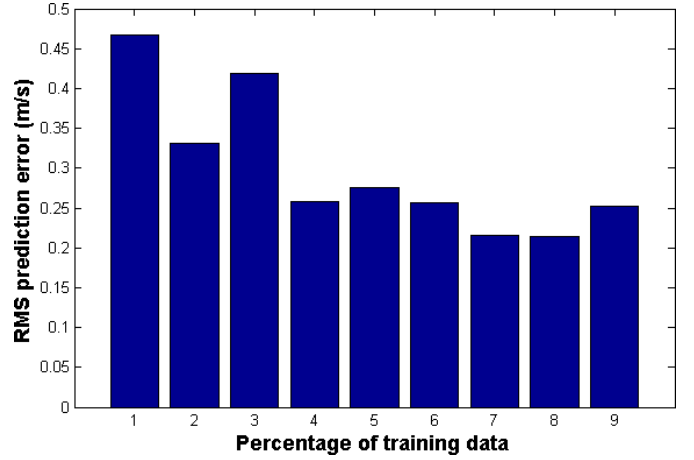


Figure 3: Illustration of errors obtained from user model with percentage of training data available. Errors reduce with increasing amount of training data. Least average error is $\approx 0.2 - 0.25$ m/s. This corresponds to an average distance error estimate of $\approx 6 \times 10^{-3}$ m for each time instant.

III. EXPERIMENTAL DESIGN

Our approach relies on the building of two complementary models. The first is the WiFi model over the floor space (as in Sec. II-B) that involves dividing the floor space into grids and collecting WiFi RSS measurements for each grid location. This model is characteristic of location and a particular time of day. It does not change from user to user. From these data a sensor model is derived. The second is the personalized user movement model (as in Sec. II-C1) that converts accelerometer information into velocity trajectories. This model changes from user to user but does not vary significantly with location or time of day.

A. Data Collection

WiFi Model: Our experiment focused on a single-floored office space consisting of rectangular hallways. This was broken into 47 grid squares (each of size $2\text{m} \times 2\text{m}$) and the center of each grid square was noted. A total of $N = 15$ APs were used. WiFi RSS measurements from each of these APs were recorded for 120 seconds per location. All measurements were taken across 5 days between 7 and 9 pm on each day to minimize the effects of interference from intermittent radio sources or people crossing. This formed the measurement model for the floor space.

Movement Model: To build user models, we collected walking information from two healthy male adults (Average age: 23 ± 1 yrs, Average height 178 ± 3 cms). Each user gave informed consent to participate. Participants were asked to wear the sensor on the left iliac crest and walk in a straight line at a self selected speed for 10 seconds while sensor data was collected on the phone. This formed one recording sample. Speeds were calculated by first measuring distance with a distance wheel and converting it to average speed by dividing it by time taken. Typical speeds were between 0.8 m/s to 1.8 m/s. Participants recorded 300 such data points with varying speeds. These data points form the training data for each user's model.

B. Movement Characterization

Our first study characterized the accuracy of the speed prediction algorithm in order to fill in parameters for the movement model. For this, each participant's dataset was randomly

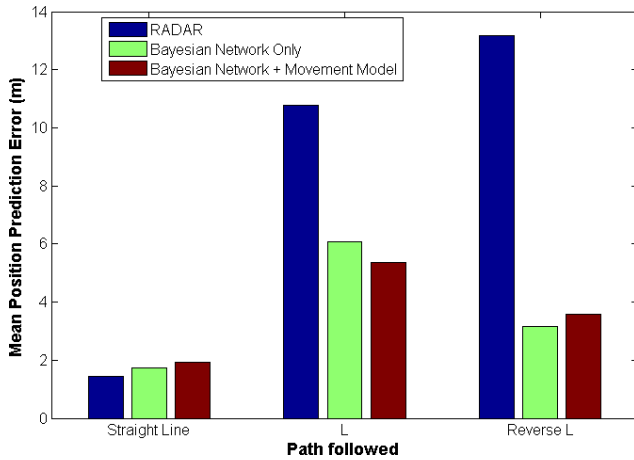


Figure 4: Illustration of position prediction errors when walking at a self-selected speed averaged across two users. The basic RADAR algorithm is used for reference. Walking in a straight line produces slightly higher error when inertial data is fused with WiFi RSS measurements. This is because of the nature of collecting ground truth involving checkpoints at grid centers. The fused algorithm performs better in cases where turns are involved. RADAR performs worst because it is not able to distinguish between two APs leading to the same distance measure from similar RSS signatures to points at the beginning leading to localization error. Position obtained from projection of inertial data helps assess the consistency of a WiFi measurement and provides less weight if the readings are far from current location. This helps counteract incorrect WiFi position measurements.

partitioned into training and testing data. The training data were used to obtain that user’s model using BLR (Sec. II-C2) and used to predict speeds on the test dataset. RMS errors were recorded. This was repeated 40 times for different randomly partitioned data and errors were averaged to obtain Average RMS errors. Similar models were built for the other user and errors averaged across users. This was repeated for different percentages of training data. Fig. 3 illustrates the effects of increasing training data on the accuracy of the model. Average RMS errors were found to reduce with increasing amount of training data. The least average error was $\approx .2 - .25$ m/s corresponding to an average distance error estimate of $\approx 6 \times 10^{-3}$ m for each time instant. This was incorporated into the noise model for the Kalman filter. This also provided insight into the minimum number of data points required to accurately characterize a user’s movement model. From this study it corresponded to approximately 60% of training data (180 data points).

C. Position Estimation

Our second study focused on the relative accuracy of fusing movement and WiFi information in the context of indoor positioning. To evaluate performance, both users recorded sensor information while walking five times in pre-defined trajectories. The two trajectories chosen were walking in a straight line and in an L-shape. Ground truth was obtained by considering a set of checkpoints and recording the time when the user crossed that particular check point. Data were then fused offline for analysis. The predicted position at the same time instant as when the users were at a check point was measured. The error was calculated as the Euclidean distance between the predicted and actual position. The effect of using only WiFi information and combining WiFi

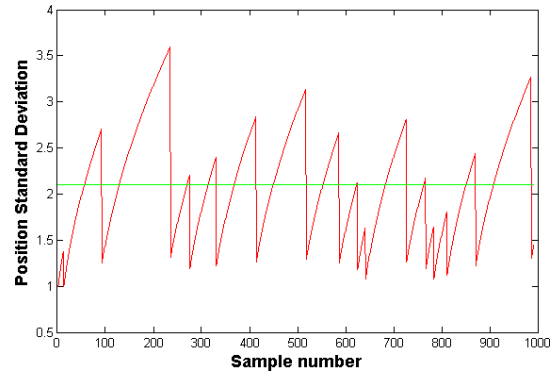


Figure 5: Illustration of position error standard deviation (shown in red) when walking at a self-selected speed for one trial run in the L-shaped trajectory. Similar plots are observed across other trajectories and both users. Regular correction from WiFi readings reduce process covariance. The mean standard deviation of position per experimental run was ≈ 2.1 m (shown in green).

with movement information was compared. For reference, a version of RADAR with 5 nearest neighbors was also used. Fig. 4 illustrates the errors obtained. Walking in a straight line produced slightly higher error when inertial data was fused with WiFi RSS measurements. This was because of the nature of collecting ground truth involving checkpoints at grid centers. If the WiFi algorithm predicted exactly at a grid center then the error for that position would be zero. The combined algorithm performed better in cases where turns are involved. This was because position obtained from projection of inertial data helps assess the consistency of a WiFi measurement when it arrives and assigns a lower weight if the measurements are far from current location. This means that a wrong WiFi reading is partially filtered providing more robust performance. This helps counteract incorrect WiFi position measurements. Walking involving a turn also requires that the user move away from the grid center. Fig. ?? illustrates two example trajectories and the predictions made. RADAR performed the worst because of its inability to distinguish between two APs that would provide the same distance measure from similar RSS signatures. Fig. ?? illustrates the error correction through WiFi as indicated by drop in variance. For the sake of intuition standard deviation is plotted instead. Similar plots are observed across other trajectories and both users. Regular correction from WiFi readings reduce process variance. In our study, the mean standard deviation in position was ≈ 2.1 m.

IV. CONCLUSION

Indoor localization has widespread applications in ubiquitous indoor monitoring, tracking and navigation -WiFi-based techniques being a natural choice. Current techniques to approach this problem such as fingerprinting or propagation model based techniques are limited in spatial resolution because of the usage of grid or graph based representations. One technique to mitigate this is to incorporate short term movement models based on on-body sensor information and fuse these measurements with long-term WiFi measurements. Mobile phones offer the advantages of both these techniques and are ubiquitous.

In this paper, we presented a data-driven probabilistic regression-based movement model for indoor, phone-based positioning through fusion with WiFi fingerprinting for one

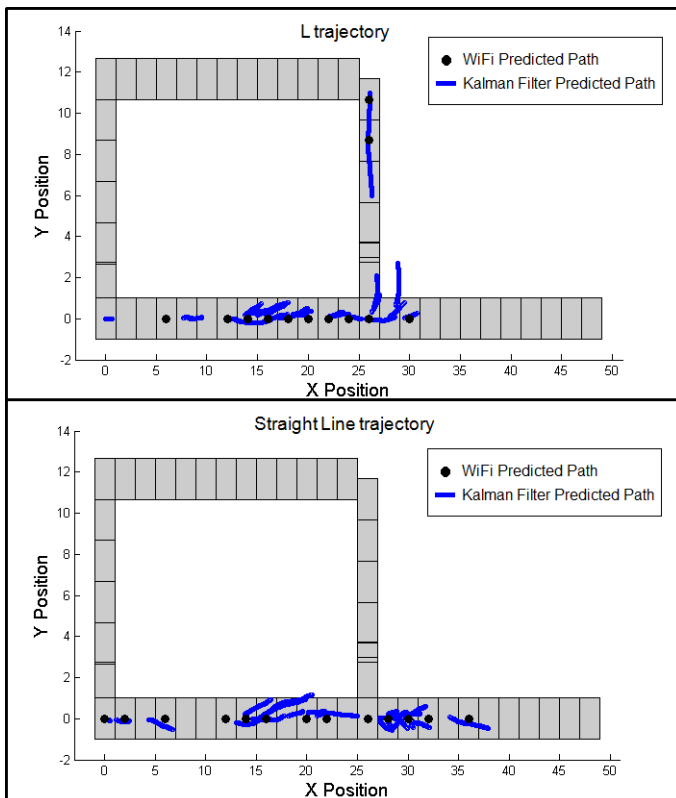


Figure 6: Illustration of predicted trajectories using WiFi alone and with Kalman Filter fused measurements from inertial sensors. Regular correction from Wi-Fi helps prevent inertial sensor drift.

dynamic activity - walking. We showed how one could use the inherent periodicity of walking to extract velocity information and use that information to obtain short term trajectories. We then fused this information with a Bayesian WiFi localization model to obtain complete trajectories. We characterized the movement model to obtain an estimate of error predictions and found that the movement model showed a best case average RMS prediction error of .25 m/s. We also presented a preliminary study characterizing combined system performance across straight line and L-shaped trajectories. The framework showed lower errors across the L-shaped trajectories. This was because position obtained from projection of inertial data helps assess the consistency of a WiFi measurement when it arrives and assigns a lower weight if the measurements are far from current location.

We plan to extend our work in a number of directions. First, we plan to incorporate angle of trajectory into the state model. Compass readings are prone to local offset variance. We will model these offsets per location and incorporate it into our building model. We also plan on adding gyroscope readings to make short term measurements of angle change. With respect to the speed estimation algorithm, we plan to improve modeling capabilities and study the effect of sensor sampling rates on prediction accuracy. We also plan on conducting a more detailed location estimation study at a higher resolution using camera information as ground truth. Using camera information as ground truth will let us branch out from straight or L-shaped paths to more generalized trajectories. Additionally, our algorithm requires a significant amount of training data to obtain subject models. However, such subject models also

share common properties across users because of the inherent similarity in walking styles across a range of people. We plan to incorporate this information using a hierarchical Bayesian model to provide informative model instantiations based on individual physical characteristics such as height, weight, age and BMI.

From the perspective of Wi-Fi readings, our approach is limited in its representation because it uses grid centers for Wi-Fi position information. Recalibration based on grid centers distorts the corrections and makes it dependent on grid dimensions. We plan on tackling this by using a particle-filter based model and also incorporate wall boundaries in a more robust manner. Our approach is also limited in that it only describes movement for one activity - walking. We plan to expand our activities to standing, sitting and walking. Present sensors on the phone already allow the recognition of user activity states. Using this activity information will allow a comprehensive movement model.

ACKNOWLEDGEMENTS

This work was supported in part by NSF (CCR-0120778) as part of the Center for Embedded Network Sensing (CENS). Support for H. Vathsangam was provided by the USC Annenberg Doctoral fellowship program.

REFERENCES

- [1] P. Bahl and V. N. Padmanabhan, "RADAR: an in-building RF-based user location and tracking system," in *INFOCOMM*, pp. 775–784, 2000.
- [2] A. Kotanen, M. Hannikainen, H. Leppakoski, and T. Hamalainen, "Positioning with IEEE 802.11b wireless LAN," in *Personal, Indoor and Mobile Radio Communications*, vol. 3, pp. 2218 – 2222, 2003.
- [3] T. Roos, P. Myllymäki, H. Tirri, P. Misikangas, and J. Sievänen, "A probabilistic approach to wlan user location estimation," *International Journal of Wireless Information Networks*, vol. 9, pp. 155–164, 2002.
- [4] M. Youssef, A. Agrawala, and A. Udaya Shankar, "WLAN location determination via clustering and probability distributions," in *Pervasive Computing and Communications*, pp. 143 – 150, 2003.
- [5] A. Haeberlen and A. Rudys, "Practical robust localization over large-scale 802.11 wireless networks," in *MOBICOM*, pp. 70–84, 2004.
- [6] J. Letchner, D. Fox, and A. LaMarca, "Large-scale localization from wireless signal strength," in *AAAI*, pp. 15–20, 2005.
- [7] P. Bahl, A. Balachandran, and V. Padmanabhan, "Enhancements to the RADAR User Location and Tracking System," 2000.
- [8] F. Evennou and F. Marx, "Advanced integration of WIFI and inertial navigation systems for indoor mobile positioning," *J. Appl. Signal Process.*, pp. 164–164, 2006.
- [9] K. Frank, B. Krach, N. Catterall, and P. Robertson, "Development and Evaluation of a Combined WLAN and Inertial Indoor Pedestrian Positioning System," *ION GNSS*, 2009.
- [10] O. Woodman and R. Harle, "Pedestrian localisation for indoor environments," in *UbiComp*, pp. 114–123, 2008.
- [11] H. Wang, H. Lenz, A. Szabo, J. Bamberger, and U. D. Hanebeck, "Wlan-based pedestrian tracking using particle filters and low-cost mems sensors," 2007.
- [12] I. Constandache, R. R. Choudhury, and I. Rhee, "Towards Mobile Phone Localization without War-Driving," *INFOCOMM*, 2010.
- [13] J.-C. Cheng and J. M. F. Moura, "Tracking Human Walking in Dynamic Scenes," in *Int. Conf. on Image Processing*, p. 137, 1997.
- [14] H. Vathsangam, A. Emken, D. Spruijt-Metz, and G. S. Sukhatme, "Toward Free-Living Walking Speed Estimation Using Gaussian Process-based Regression with On-Body Accelerometers and Gyroscopes," in *ICST 4th International ICST Conference on Pervasive Computing Technologies for Healthcare*, 2010.
- [15] L. Bao and S. S. Intille, "Activity Recognition from User-Annotated Acceleration Data," *Pervasive Computing*, pp. 1–17, 2004.
- [16] D. W. Grieve and J. Ruth, "The Relationships Between Length of Stride, Step Frequency, Time of Swing and Speed of Walking for Children and Adults," *Ergonomics*, vol. 9, pp. 379–399, 1966.
- [17] Z. Sun, X. Mao, W. Tian, and X. Zhang, "Activity classification and dead reckoning for pedestrian navigation with wearable sensors," *Measurement Science and Technology*, vol. 20, no. 1, 2009.
- [18] C. M. Bishop, *Pattern Recognition and Machine Learning*. Information Science and Statistics, 2008.